Ceramics International 44 (2018) 5629–5635

Contents lists available at ScienceDirect

Ceramics International

journal homepage: www.elsevier.com/locate/ceramint

Improved toughness of layered architecture TiAlN/CrN coatings for titanium high speed cutting

Xudong Sui[a,b], Guojian Li[a,*], Chenjie Jiang[a], Kai Wang[a], Yingjie Zhang[c], Junying Hao[b], Qiang Wang[a]

[a] Key Laboratory of Electromagnetic Processing of Materials (Ministry of Education), Northeastern University, Shenyang 110004, China
[b] State Key Laboratory of Solid Lubrication, Lanzhou Institute of Chemical Physics, Chinese Academy of Science, Lanzhou 730000, China
[c] College of Sciences, Northeastern University, Shenyang 110004, China

ARTICLE INFO

Keywords:
Layered design
Fracture toughness
Bilayer period
Titanium cutting

ABSTRACT

Fracture toughness is an important characteristic for coatings for high speed cutting of titanium. This study focuses on improving the fracture toughness of the coatings using a layered design method. TiAlN/CrN multilayer coatings with bilayer periods between 12 nm and 270 nm were prepared by reactive magnetron sputtering. XRD results show the multilayer coatings have face-centred cubic structures. When the bilayer period of multilayer coating decreases from 270 nm to 25 nm, the coating hardness decreases from 24.5 GPa to 18.1 GPa. Increased fracture toughness and adhesion strength of multilayer coatings are observed with decreasing bilayer periods. A maximum fracture toughness (K_{IC}) of 3.6 MPa $m^{1/2}$ and adhesion strength of 107 N were obtained with a 25 nm bilayer period. The inhibition of crack propagation is the main reason for the high fracture toughness values in multilayer coatings. However, when the bilayer period is decreased further (12 nm), the coating hardness begins to increase rapidly to 23.4 GPa, and the fracture toughness and adhesion strength begin to decrease. Titanium cutting results show that an improvement in cutting performance is obtained with a TiAlN/CrN_25 multilayer coating.

1. Introduction

Titanium alloys have been widely used in many industrial fields, including the aeronautic, automotive and biological industries [1]. However, machining of titanium alloys is still a challenge. Serious tool vibration is one of the most critical issues during alloy machining because of titanium's low elastic modulus [2–4]. Tool vibration will accelerate crack propagation at the tip, which will result in reduced cutting performance. This problem becomes more severe during high speed machining of titanium alloys. Therefore, it is important to improve the coating toughness for tools for machining titanium alloys.

Physical vapor deposition (PVD) is a widely used method of coating tools to improve their cutting performance. It is well known that metal nitride hard coatings can improve the lifetime and cutting performance of cutting tools. For example, TiAlN coating has been widely used in many cutting operations due to its high hardness and wear resistance [5–8]. CrN coatings have high oxidation temperatures and excellent corrosion resistances [9,10]. However, it is difficult for a single coating to meet the requirements for the high speed machining of titanium, so many methods have been developed to improve the mechanical properties of the coatings. One successful advance in the coating industry was the implementation of multilayered architectures [11–14]. Multilayer structural design has attracted much attention in improving the performance of metal/metal, metal/ceramic and ceramic/ceramic coatings [15–18]. Previous studies on TiAlN/CrN coatings have shown that a layered design is an effective way to give coating excellent mechanical and thermal properties [19,20]. In addition, the improved coating performance is closely related with the bilayer period of multilayer coatings. The influence of the bilayer period on the microstructure and mechanical properties of multilayered coatings has been well studied. However, previous studies have mostly focus on bilayer periods below 50 nm. Thicker bilayer periods have rarely been reported. Generally, most of studies (bilayer period < 50 nm) have shown that the hardness of the coating increases first and then decreases as the bilayer period increases (0–50 nm) [21–23]. However, recent study has found that when continues to increase the bilayer period (> 50 nm), the hardness of the coating may also be on the rise [24]. Therefore, the effect of thicker bilayer periods (> 50 nm) on the mechanical properties of the coating needs further study. In this study, TiAlN/CrN coatings with relatively large bilayer periods, between 12 nm and 270 nm,

* Corresponding author.
E-mail address: gjli@epm.neu.edu.cn (G. Li).

https://doi.org/10.1016/j.ceramint.2017.12.210
Received 10 September 2017; Received in revised form 21 December 2017; Accepted 28 December 2017
Available online 30 December 2017

Table 1
Deposition time for the different layers of multilayer coatings.

Coatings	Buffer layer (min)		Multilayer structure (min)		Bilayer period (nm)
	Cr	CrN	CrN	TiAlN	
Sample 1	5.0	5.0	0.25 × 216	0.25 × 215	≈ 12
Sample 2	5.0	5.0	0.50 × 108	0.50 × 107	≈ 25
Sample 3	5.0	5.0	1.00 × 54	1.00 × 53	≈ 52
Sample 4	5.0	5.0	3.00 × 18	3.00 × 17	≈ 150
Sample 5	5.0	5.0	6.00 × 9	6.00 × 8	≈ 270

Table 2
Cutting parameters for titanium cutting test.

Machining operation	Tool substrate	Speed (m/min)	Depth of cut (mm)	Feed (mm/rev)
Longitudinal turning	WC-Co, CNMG120408	100	0.5	0.2

were prepared by reactive magnetron sputtering. The effect of the bilayer period on the coating microstructure and mechanical properties has been studied. Furthermore, the titanium cutting performance of these coatings was evaluated by a titanium cutting experiment.

2. Experimental details

Multilayered TiAlN/CrN coatings were prepared on cemented carbide (YG8,Co = 8 wt%) and commercial n-type Si (100) wafer substrates using reactive magnetron sputtering. The magnetron sputtering device was equipped with four 3.5-in. targets. The substrates were first polished with diamond abrasive discs and then with 2.5 μm diamond pastes until smooth surfaces with roughnesses of Sq ≈ 10 nm were obtained. Then, the substrates were sequentially cleaned with acetone and ethanol in an ultrasonic cleaner. The pre-treatment method is identical to those of our previous report [25].

After the base pressure reached 3×10^{-3} Pa, the substrate was heated to 400 °C. A pure Cr target (99.99%) and a $Ti_{0.50}Al_{0.50}$ alloy target (99.9%) were used to prepare alternating CrN and TiAlN layers, respectively. All targets were cleaned by sputtering in pure argon gas for 5 min before depositing the coatings. Pure Cr and CrN buffer layers were first sequentially deposited at an argon pressure of 0.5 Pa for 5 min. Then, the total work pressure was maintained at 0.5 Pa with $P_{N2}/(P_{Ar}+P_{N2}) = 30\%$. Alternating coatings of CrN and TiAlN were deposited. The CrN layers were deposited with a pure Cr target power of 900 W. The $Ti_{0.50}Al_{0.50}$ target was operated at 900 W to deposit the TiAlN layer. The deposition time of each layer was controlled by the switching time of the target baffles. Thus, multilayer coatings with different bilayer periods were obtained, as shown in Table 1.

The morphologies and thicknesses of the coatings were characterized by scanning electron microscopy (SEM, SUPRA 35). An energy dispersive spectrometer (EDS, OXFORD) was used to evaluate the chemical composition. The crack propagation behaviour was observed by transmission electron microscopy (TEM, TECNAI G2 F30). Structural investigations were performed with glazing incidence X-ray diffraction (GIXRD, D/MAX 2400) with diffraction angles between 30° and 80° and an incident angle of 3°. The wavelength of the CuKα radiation was 0.154 nm. Surface roughness was determined with an atomic force microscope (AFM, NANOSURF C3000). The hardness of the coatings was determined by a nanoindenter (AGILENT, G200) with an indentation depth of approximately 200 nm and a Poisson's ratio of 0.23. Due to the lack of an effective method for evaluating the fracture toughness of the hard coating material, an indentation method to is usually used to evaluate fracture toughness for reference. In this paper, the coating fracture toughness was measured with a Vickers hardness tester (FUTRUE-TECH, FM-800) under a load of 100 g. The fracture toughness (K_{IC}) of the deposited coatings is calculated by the following equation [26–28]:

$$K_{IC} = \delta\left(\frac{P}{C^{3/2}}\right)\sqrt{\frac{E}{H}} \quad (1)$$

where P is the applied load; δ is the indenter geometry constant, which is equal to 0.016 for a Vickers diamond pyramid indenter; E and H are the elastic modulus and hardness, which can be calculated directly from the indentation analysis; and C is the radial crack length emanating from the corners of the sharp indenter.

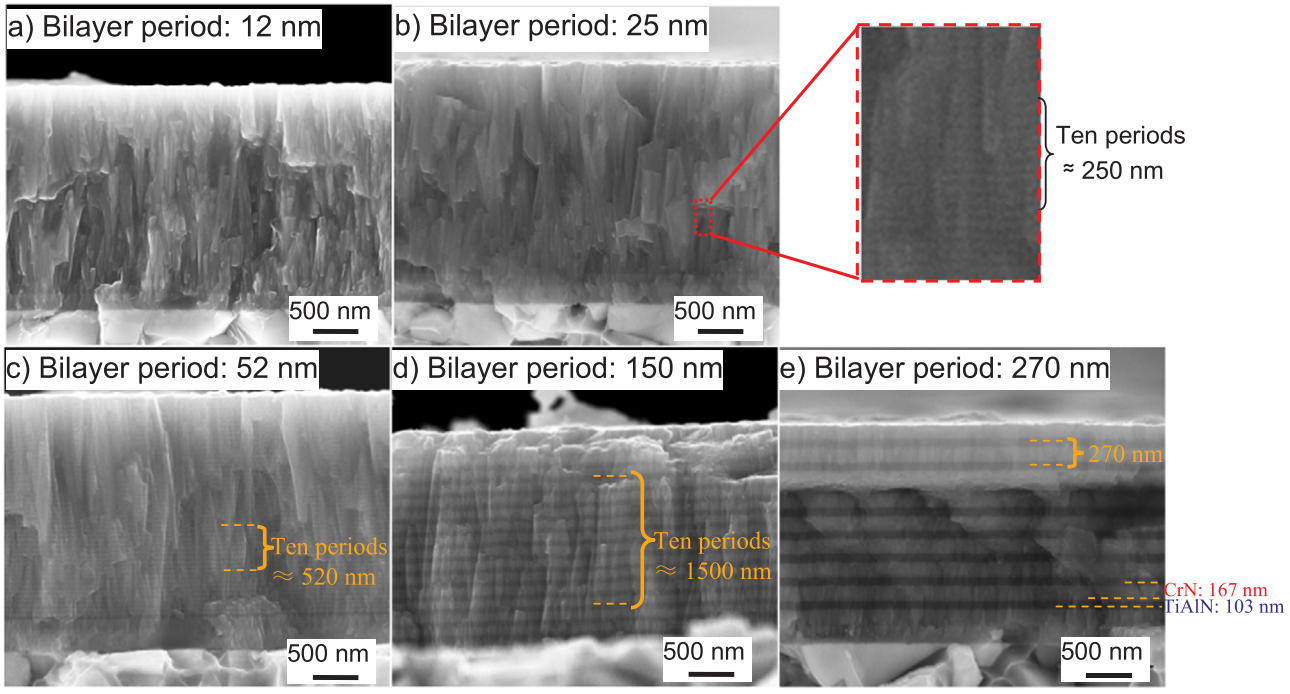

Fig. 1. Cross-section SEM images of the TiAlN/CrN coatings with different bilayer periods.

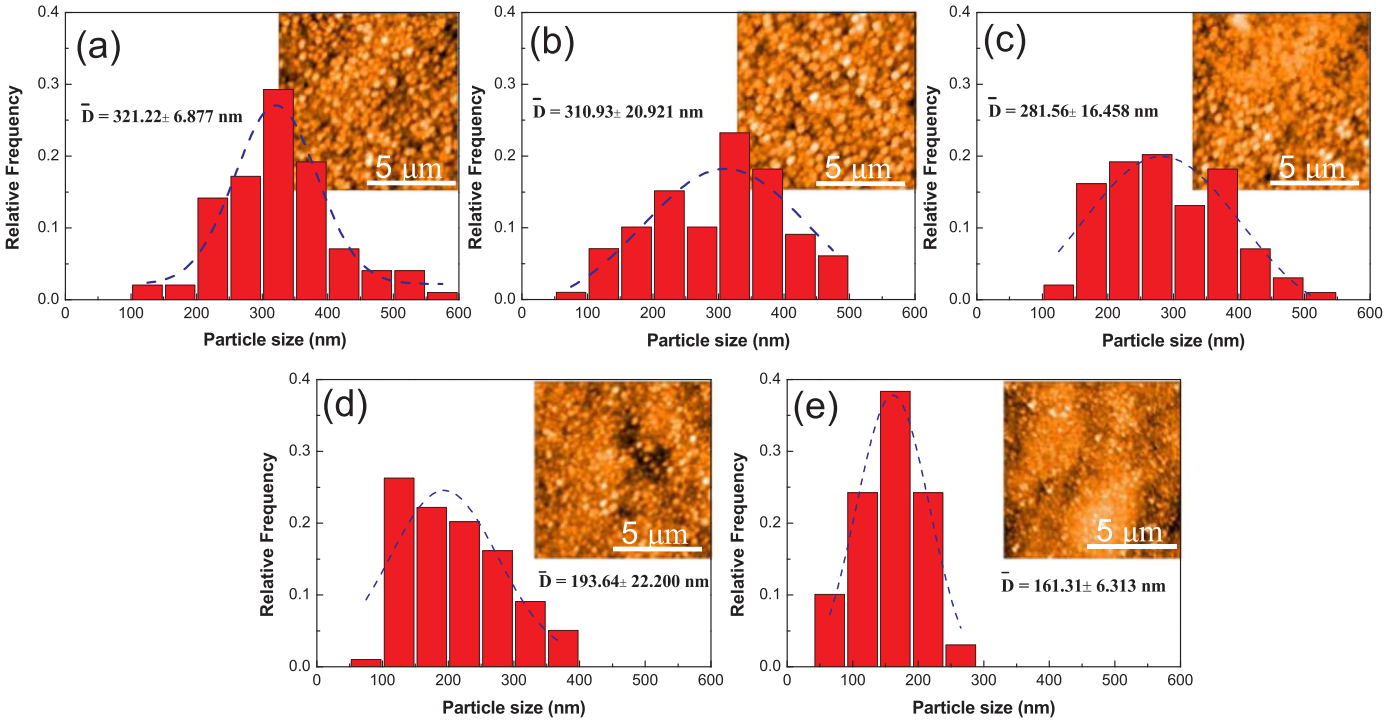

Fig. 2. Particle size distribution of the TiAlN/CrN coatings with different bilayer periods. 12 nm (a); 25 nm (b); 52 nm (c); 150 nm (d); and 270 nm (e). The inserts are the surface AFM images of the corresponding TiAlN/CrN coatings.

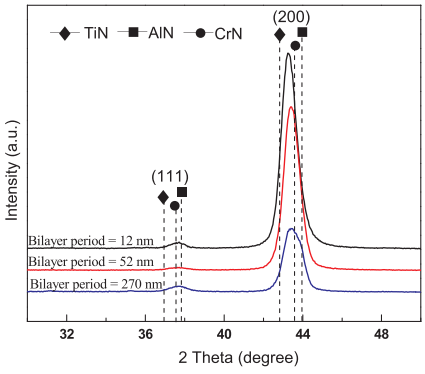

Fig. 3. XRD patterns of the TiAlN/CrN coatings with different bilayer periods.

The adhesion strength was tested with a scratch tester (MFT-4000) at a loading rate of 100 N/min and a scratch length of 5 mm. Indentation and scratch morphologies were observed by optical microscopy (OLYMPUS, DSX500). Titanium turning tests were conducted on a CNC lathe (MAZAK® INTEGREX 200Y). A coolant was applied during the testing. Cutting parameters are listed in Table 2.

3. Results and discussion

3.1. Coating structure and morphology

The fracture cross-section morphologies of TiAlN/CrN multilayer coatings were observed by SEM, as shown in Fig. 1. The thickness of our coatings ranged from 2.4 μm to 2.7 μm. As shown in Fig. 1e, the dark layer is the TiAlN coating, and the light-coloured layer is the CrN coating. The thickness ratio between the CrN and the TiAlN layers is 1.62. Since the deposition time of TiAlN and CrN is increased proportionally, we can assume the thickness ratio of the TiAlN to the CrN layers is constant and approximately equal to 1.62 in all cases. From Fig. 1b to 1e, we can clearly see that the bilayer periods of the TiAlN/CrN multilayer coatings are approximately 25, 52, 150 and 270 nm. The bilayer period of ~ 12 nm for the TiAlN/CrN multilayer coating (Fig. 1a) was calculated according to the deposition rate of TiAlN and CrN. For convenience, we use TiAlN/CrN_270 to represent the TiAlN/CrN multilayer coatings with a bilayer period of 270 nm in the subsequent discussion.

High-magnification SEM images of the TiAlN/CrN coatings with small bilayer periods mainly show the columnar morphology. As the bilayer period decreases, the columnar characteristic of the coatings

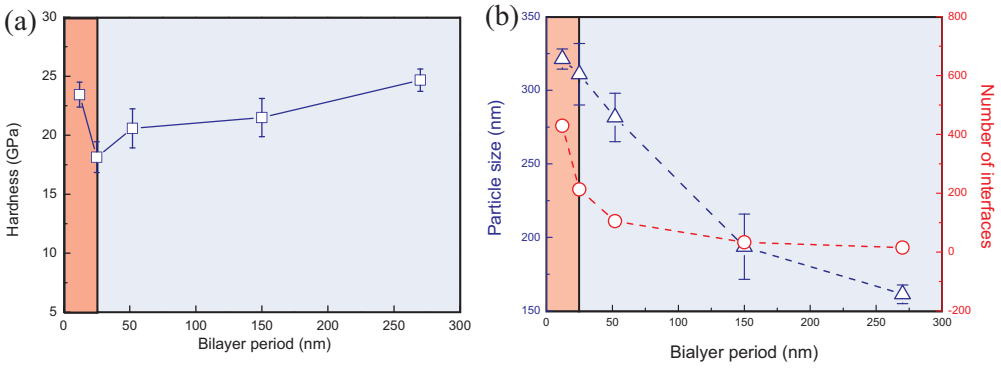

Fig. 4. Hardness, particle size and interface number of the TiAlN/CrN coatings with different bilayer periods.

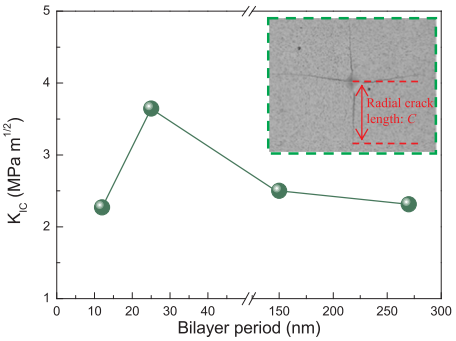

Fig. 5. Fracture toughness of the TiAlN/CrN coatings with different bilayer periods.

becomes insignificant. When the bilayer period increases to 270 nm, the TiAlN/CrN_270 coating is closer to exhibit a fine-grain structure. This cross-sectional morphology change is consistent with the trends observed in the surface AFM images of the TiAlN/CrN coatings. The calculated particle size distributions from the AFM images are presented in Fig. 2. The surface particle generally composed by several adjacent columnar grains. This leads to that the surface particle size in Fig. 2 is larger than the size of columnar grains in Fig. 1. Although the surface particle size is not identical to the columnar grain size inside the coating, it can reflect the relation between the columnar grain and the surface particle in a certain extent.

The XRD patterns of multilayer coatings are shown in Fig. 3. There is only a set of (111) and (200) diffraction peaks, suggesting that our coatings have face-centred cubic (fcc) structures. This is because the TiAlN and CrN coatings have fcc structures, and they have a template effect on each other [29]. Therefore, due to the small mismatch between lattice parameters, coherent epitaxial growth occurs easily at small the bilayer periods [29,30]. In this case, the coating tends to grow into large columnar crystals. In addition, the intensity of the diffraction peaks is also stronger at the small bilayer period. Therefore, the smaller the bilayer thickness is, the better the crystallinity. This is consistent with the statistical results of particle size shown in Fig. 2. In this study, the grain size is related to the columnar growth because the continuous growth of columnar crystals inside the coating may be interrupted by the presence of thicker CrN layers. Reducing the bilayer period is easy to make the coating prone to template growth and otherwise the coating is not template growth. That is to say, the coating exhibits a fine-grain structure without template growth effect (Fig. 1e) and results in a large columnar structure for template growth. Thus, the grain size of multilayer coatings increases as the bilayer period decreases in the bilayer period range studied in this work.

3.2. Hardness

The hardnesses of the TiAlN/CrN coatings are presented in Fig. 4. The hardness curve exhibits “V” type as show in Fig. 4. When the bilayer period decreases from 270 to 25 nm, the coating hardness decreases from 24.5 GPa to 18.1 GPa (blue region in Fig. 4). However, continue to reduce the bilayer period, the hardness of the coatings increases rapidly to 23.4 GPa (red region in Fig. 4). Generally, the hardness of sputtered coatings is mainly decided by the size of the columnar crystals. The hardness is usually inversely proportional to the grain size according to the Hall-Petch formula. However, the effect of the interfaces on the hardness of the coating is also important in multilayer coatings. The more interfaces will cause a higher hardness. Therefore, the hardness of our multilayer coatings can be explained by two factors: particle size and interface number.

Fig. 4b shows the variation of the particle size and interface number with the bilayer period. When the bilayer period decreases from 270 to 25 nm, as shown in the blue region of Fig. 4b, the particle size of the coatings increases quickly from 161 to 310 nm. At the same time, the number of interfaces in the coatings increases slowly. So, the hardness of the coating in this region is primly controlled by grain refinement mechanism. However, when the bilayer period continues to drop to 12 nm, as shown in the red region of Fig. 4b, the number of interfaces in the coating increases dramatically. The increase in particle size is within the error range. As a result, the effect of the interface strength mechanism is enhanced and the hardness of the coating changes to increase. Other explanation for this phenomenon is the dislocation-based mechanism proposed by Chu and Barnett [31] or a combined effects of a superlattice effect, the coherency strain effects and the Koehler models [11,32–34]. The stresses required for dislocations to glide across layers with different shear modulus are larger at small bilayer periods.

3.3. Fracture toughness

The fracture toughnesses (K_{IC}) of the TiAlN/CrN coatings deposited on the Si (100) substrates were calculated from Eq. (1) (shown in Fig. 5). An increase in fracture toughness of the multilayer coatings is observed when the bilayer period decreases from 270 to 25 nm. A maximum K_{IC} value of approximately 3.6 MPa $m^{1/2}$ is obtained at a bilayer period of 25 nm. This trend is consistent with previous studies on TiAlN/CrSiN multilayer coatings [28]. Generally, the fracture toughness of sputtered coatings is inversely proportional to the hardness. However, the interface effect also has a significant effect on toughness in multilayer coating system. Phenomena such as crack deflection, energy dissipation, and stress relaxation occurs at the interface often helps to improve the toughness of the coatings [15,28,35].

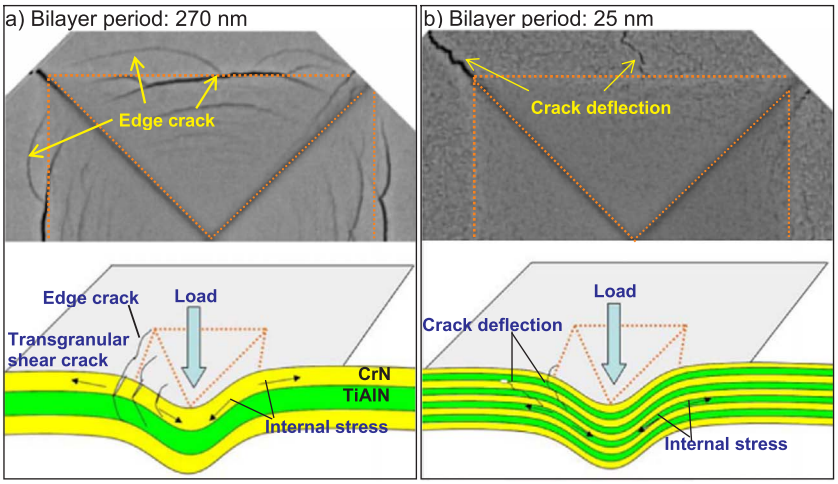

Fig. 6. Indentation morphology and schematic of the TiAlN/CrN coatings with different bilayer periods.

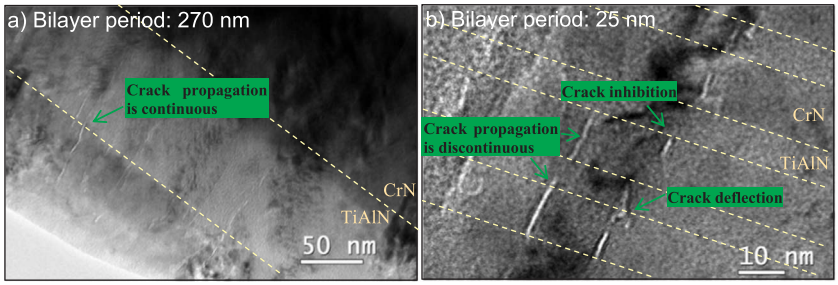

Fig. 7. Cross-section TEM images of the TiAlN/CrN coatings with different bilayer periods.

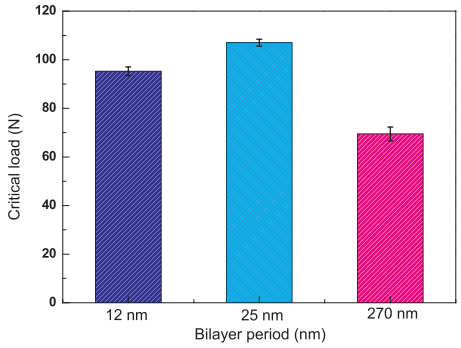

Fig. 8. Critical load of TiAlN/CrN coatings with different bilayer periods.

Therefore, when the bilayer period decreases from 270 nm to 25 nm, the reason for the increase of coating toughness is mainly due to the decrease of hardness and the increase of interface quantity (blue region in Fig. 4). The highest fracture toughness of TiAlN/CrN_25 coating is owing to its lowest hardness and relatively more interface. However, as the bilayer period is further reduced to 12 nm, the hardness of TiAlN/CrN_12 coating increases rapidly. The high hardness will significantly reduce the toughness of the coating. In addition, although the number of interfaces of the TiAlN/CrN_12 coating is increased, the interface becomes more noticeable (Fig. 1). This will also be harmful to the coating toughness. So the toughness of TiAlN/CrN_12 coating is reduced.

To study the effect of multilayer design on fracture toughness, the indentation morphologies of TiAlN/CrN coatings with bilayer periods of 270 nm and 25 nm were observed by SEM, as shown in Fig. 6. The corresponding indentation morphology schematic is also presented in Fig. 6. When a load is applied to the coating, it will produce internal stress in the multilayer coatings at the edge of the indentation (Fig. 6). When the bilayer period is large (270 nm, Fig. 6a), it is easy to produce a serious transgranular shear crack in the coating under this internal stress [36]. Thus, deep and straight edge cracks tend to be formed at the edges of the indentation (see Fig. 6a). However, with decreased bilayer periods, the number of interfaces in the coatings increase, which leads to crack deflection at the interfaces [37]. Thus, small and bent cracks tend to be formed at the edges of the indentations (see Fig. 6b). This is the main reason for the high fracture toughness of TiAlN/CrN_25

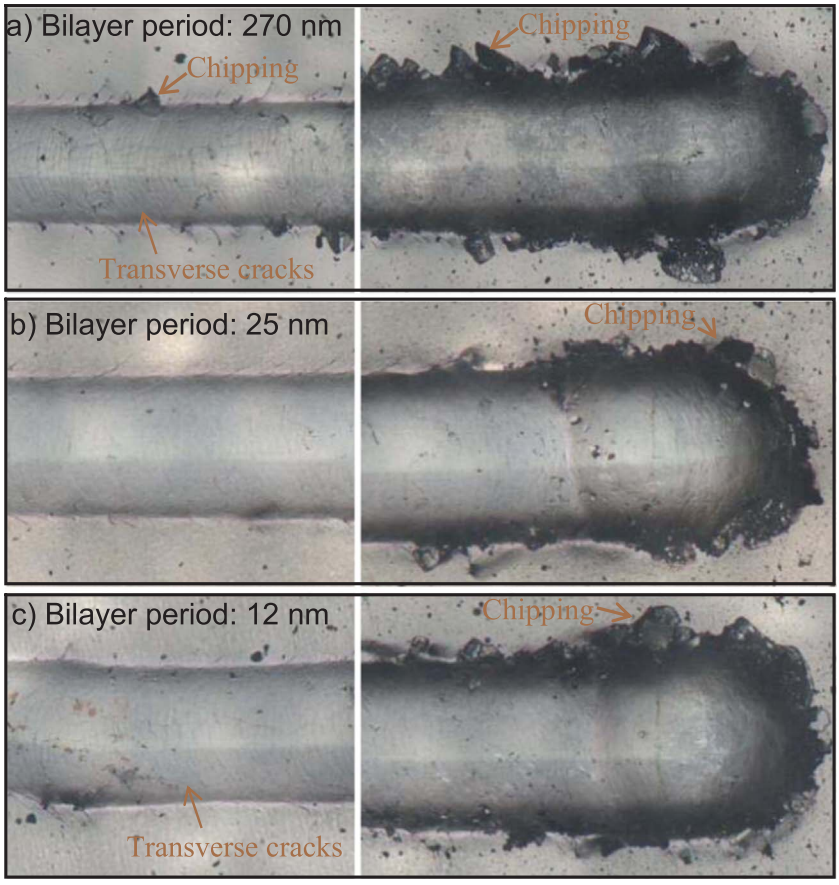

Fig. 9. Scratches in the TiAlN/CrN coatings with different bilayer periods at loads of 55 N and 100 N.

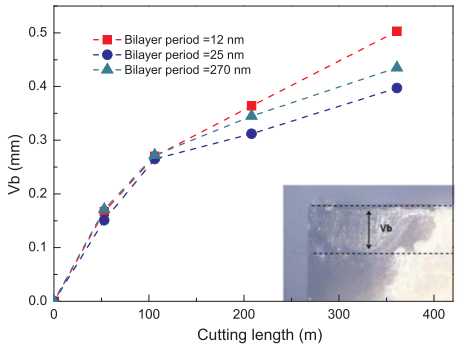

Fig. 10. Tool flank wear (Vb) on various multilayer-coated tools after turning Ti6Al4V at 100 m/min.

coatings.

The crack propagation behaviour in multilayer coatings can also be observed by TEM as shown in Fig. 7. When the bilayer period is 270 nm, the cracks deflect only slightly at the interface, and crack propagation is continuous (see Fig. 7a). It is easy for the cracks to extend into the internal crystal. As a result, the cracks formed in the coatings are long and straight. When decreasing the bilayer period to 25 nm, the number of interface increases, and the crack propagation is inhibited and deflected at the interfaces. Cracks formed in the coatings are discontinuous and bent. The ability of a multilayer design to inhibit crack propagation improves the fracture toughness of the coating.

3.4. Adhesion

The results of the scratch tests are shown in Fig. 8. All coatings exhibited good adhesion with minimum critical loads of not less than 60 N. The good adhesion strengths of these coatings can be attributed to the presence of the Cr and CrN interlayers [19]. As the bilayer period decreases, the coating adhesion strength peaks at 107 N at a bilayer period of 25 nm, and then it decreases to 95 N at a bilayer period of 12 nm. This is consistent with the observed scratch morphology. At a load of approximately 55 N, deep, obvious transverse cracks occurred along the scratch track of the TiAlN/CrN_270 coating (Fig. 9a). Chips in the coating also appeared on both sides of the scratch track. However, the number of transverse cracks and chips decreased gradually as the bilayer period decreased. The transverse cracks and chips disappeared from the scratch track at a load of 55 N when the bilayer period decreased to 25 nm (Fig. 9b). The decrease in the number of transverse cracks and chips is mainly related to an increased interface enhancement effect due to a decrease in the bilayer period, which can improve the adhesion strength. As the bilayer period is further reduced to 12 nm, the number of transverse cracks in the coating decreased slightly, but no obvious chipping was observed on either side of the scratch track (Fig. 9c). At a higher load of 100 N, chipping occurred on all multilayered coatings. However, spallation of the coatings did not occur, and no total delamination was observed in scratch track.

3.5. Titanium cutting results

Fig. 10 shows a comparison of tool wear on coated inserts for continuous turning of a titanium alloy (TC4) at a cutting speed of 100 m/min with coolant. Tool wear was evaluated by measuring the average flank wear land width (Vb) as shown in the inserts of Fig. 10. Since the titanium alloy is difficult to machine due to its low elastic modulus, high chemical affinity, and low thermal conductivity, the coater inserts has already severely damaged after high speed cutting titanium as shown in Fig. 11. According to the cutting results, the coating flaking of the TiAlN/CrN_25 coating occurs less than that of the other two coatings and the cracks generated inside the coating are well suppressed. This means that the TiAlN/CrN_25 coating has the best performance. Generally, the cutting performance of coatings is closely related to its adhesion, toughness, hardness, oxidation resistance and so on. Meanwhile, in this study, the TiAlN/CrN_25 coating has the lowest hardness, the highest critical load and fracture toughness. Thus, it is reasonable that the good toughness and high adhesion strength may play more important role in obtaining good cutting performance except for hardness, oxidation resistance and red hardness [38]. This may be mainly due to the severe tool wear and chatter during cutting titanium alloy.

4. Conclusions

In this work, TiAlN/CrN multilayer coatings with a large range of bilayer periods, 12–270 nm, were prepared by reactive magnetron sputtering. XRD results show that the multilayer coatings have face centred cubic (fcc) structures. The effect of the bilayer period on the coating microstructure and the mechanical and cutting properties has been studied. When the bilayer period is large (thickness = 25–270 nm), the coating hardness decreases from 24.5 to 18.1 GPa as the bilayer period decreases. The decreased hardness is mainly controlled by a grain refinement mechanism. Increased fracture toughness and adhesion strength of the multilayer coatings are observed with decreasing bilayer periods. A maximum K_{IC} of 3.6 MPa $m^{1/2}$ and adhesion strength of 107 N were obtained with a 25 nm bilayer period. The crack propagation inhibition caused by the multilayer design is the main reason for the increase in the fracture toughness. As the bilayer period continued to decrease (12 nm), the coating hardness increases with decreasing bilayer period. The fracture toughness and adhesion

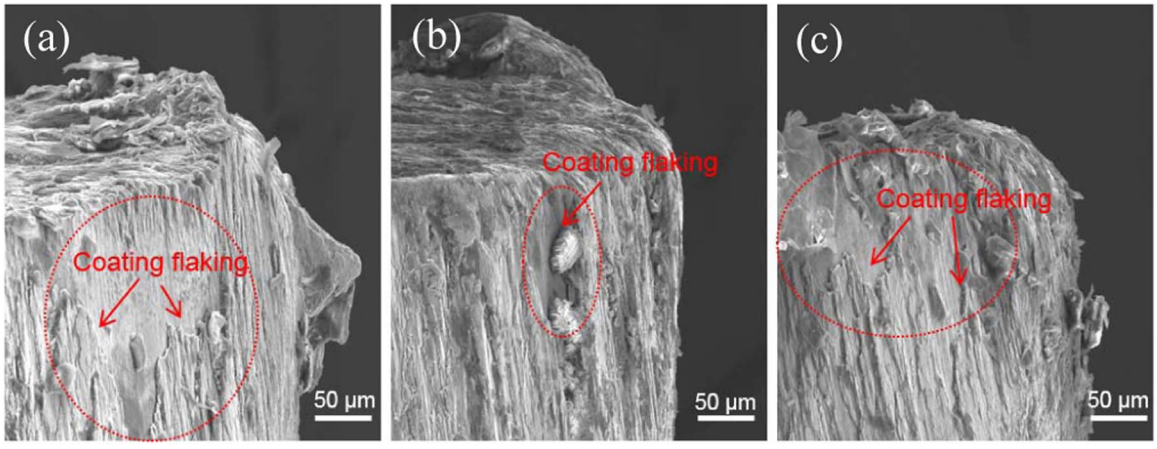

Fig. 11. SEM morphology of worn coated tools after turning Ti6Al4V at 100 m/min. 12 nm (a); 25 nm (b); 270 nm (c).

strength begins to decrease as well. Titanium cutting results show that an improvement in cutting performance is obtained with a TiAlN/CrN_25 multilayer coating.

Acknowledgements

The authors gratefully acknowledge the financial support of the National Science and Technology Major Project (2012ZX04003061) and the Fundamental Research Funds for the Central Universities (Grant No. N140503003).

References

[1] J. Davim, Machining of Titanium Alloy, Springer, 2014.
[2] A. Biksa, K. Yamamoto, G. Dosbaeva, S.C. Veldhuis, G.S. Fox-Rabinovich, A. Elfizy, T. Wagg, L.S. Shuster, Wear behavior of adaptive nano-multilayered AlTiN/MexN PVD coatings during machining of aerospace alloys, Tribol. Int. 43 (2010) 1491–1499.
[3] J.A. Ghani, C.H.C. Haron, S.H. Hamdan, A.Y.M. Said, S.H. Tomadi, Failure mode analysis of carbide cutting tools used for machining titanium alloy, Ceram. Int. 39 (2013) 4449–4456.
[4] G.J. Li, X.D. Sui, C.J. Jiang, Y. Gao, K. Wang, Q. Wang, D. Li, Low adhesion effect of TiAlTaN/TaO functional composite coatings on the titanium cutting performance of coated cemented carbide inserts, Mater. Des. 110 (2016) 105–111.
[5] S. PalDey, S.C. Deevi, Single layer and multilayer wear resistant coatings of (Ti,Al)N: a review, Mat. Sci. Eng. 342 (2003) 58–79.
[6] J. Todt, R. Pitonak, A. Köpf, R. Weißenbacher, B. Sartory, M. Burghammer, R. Daniel, T. Schöberl, J. Keckes, Superior oxidation resistance, mechanical properties and residual stresses of an Al-rich nanolamellar $Ti_{0.05}Al_{0.95}N$ coating prepared by CVD, Surf. Coat. Tech. 258 (2014) 1119–1127.
[7] Y. Long, J.J. Zeng, D.H. Yu, S.H. Wu, Microstructure of TiAlN and CrAlN coatings and cutting performance of coated silicon nitride inserts in cast iron turning, Ceram. Int. 40 (2014) 9889–9894.
[8] S.S. Zhao, H. Du, J.D. Zheng, Y. Yang, W. Wang, J. Gong, C. Sun, Deposition of thick TiAlN coatings on 2024 Al/SiCp substrate by arc ion plating, Surf. Coat. Tech. 202 (2008) 5170–5174.
[9] L. Hultman, Thermal stability of nitride thin films, Vacuum 57 (2000) 1–30.
[10] Y.X. Qiu, S. Zhang, J.W. Lee, B. Li, Y.X. Wang, D.L. Zhao, Self-lubricating CrAlN/VN multilayer coatings at room temperature, Appl. Surf. Sci. 279 (2013) 189–196.
[11] P.C. Yashar, W.D. Sproul, Nanometer scale multilayered hard coatings, Vacuum 55 (1999) 179–190.
[12] P. Angerer, J.M. Lackner, M. Wiessner, G.A. Maier, L. Major, Thermal behaviour of chromium nitride/titanium–titanium carbonitride multilayers, Thin Solid Films. 562 (2014) 159–165.
[13] L. Chen, Y.X. Xu, Influence of interfacial structure on the mechanical and thermal properties of CrAlN/ZrN multilayer coatings, Mater. Des. 106 (2016) 1–5.
[14] Y.Y. Chang, C.J. Wu, Mechanical properties and impact resistance of multilayered TiAlN/ZrN coatings, Surf. Coat. Technol. 231 (2013) 62–66.
[15] J.Y. Zhang, G. Liu, X. Zhang, G.J. Zhang, J. Sun, E. Ma, A maximum in ductility and fracture toughness in nanostructured Cu/Cr multilayer films, Scritpa. Mater. 62 (2010) 333–336.
[16] S. Kaciulis, A. Mezzi, G. Montesperelli, F. Lamastra, M. Rapone, F. Casadei, T. Valente, G. Gusmano, Multi-technique study of corrosion resistant CrN/Cr/CrN and CrN:C coatings, Surf. Coat. Technol. 201 (2006) 313–319.
[17] R. Ali, M. Sebastiani, E. Bemporad, Influence of Ti-TiN multilayer PVD-coatings design on residual stresses and adhesion, Mater. Des. 75 (2015) 47–56.
[18] J.H. Lee, W.M. Kim, T.S. Lee, M.K. Chung, B.K. Cheong, S.G. Kim, Mechanical and adhesion properties of Al/AlN multilayered thin films, Surf. Coat. Technol. 220 (2000) 133–134.
[19] B. Warcholinski, A. Gilewicz, Mechanical properties of multilayer TiAlN/CrN coatings deposited by cathodic arc evaporation, Surf. Eng. 27 (2011) 491–497.
[20] H.C. Barshilia, M.S. Prakash, A. Jain, K.S. Rajam, Structure, hardness and thermal stability of TiAlN and nanolayered TiAlN/CrN multilayer films, Vacuum 77 (2005) 169–179.
[21] C.M. Kao, J.W. Lee, H.W. Chen, Y.C. Chan, J.G. Duh, S.P. Chen, Microstructures and mechanical properties evaluation of TiAlN/CrSiN multilayered thin films with different bilayer periods, Surf. Coat. Techol. 205 (2010) 1438–1443.
[22] K.J. Martin, A. Madan, D. Hoffman, J. Ji, S.A. Barnett, Mechanical properties and thermal stability of TiN/TiB_2 nanolayered thin films, J. Vac. Sci. Technol. A. 23 (2005) 90–98.
[23] L. Chen, Y.X. Xu, Y. Du, Y. Liu, Effect of bilayer period on structure, mechanical and thermal properties of TiAlN/AlTiN multilayer coatings, Thin Solid Films 592 (2015) 207–214.
[24] Y.Q. Wei, X.Y. Zong, Z.Q. Jiang, X.B. Tian, Characterization and mechanical properties of TiN/TiAlN multilayer coatings with different modulation periods, Int. J. Adv. Manuf. Technol. 3 (2017) 1–7.
[25] X.D. Sui, G.J. Li, X.S. Qin, H.D. Yu, X.K. Zhou, K. Wang, Q. Wang, Relationship of microstructure, mechanical properties and titanium cutting performance of TiAlN/TiAlSiN composite coated tool, Ceram. Int. 42 (2016) 7524–7532.
[26] A. Karimi, Y. Wang, T. Cselle, M. Morstein, Fracture mechanisms in nanoscale layered hard thin films, Thin Solid Films. 420 (2002) 275–280.
[27] P. Jedrzejowski, J.E. Klemberg-Sapieha, L. Martinu, Relationship between the mechanical properties and the microstructure of nanocomposite TiN/$SiN_{1.3}$ coatings prepared by low temperature plasma enhanced chemical vapor deposition, Thin Solid Films. 426 (2003) 150.
[28] M.K. Wu, J.W. Lee, Y.C. Chan, H.W. Chen, J.G. Duh, Influence of bilayer period and thickness ratio on the mechanical and tribological properties of CrSiN/TiAlN multilayer coatings, Surf. Coat. Technol. 206 (2011) 1886–1892.
[29] J.L. Lin, N.Y. Zhang, Z.L. Wu, W.D. Sproul, M. Kaufman, M.K. Lei, J.J. Moore, Thick CrN/AlN superlattice coatings deposited by the hybrid modulated pulsed power and pulsed dc magnetron sputtering, Surf. Coat. Technol. 228 (2013) 601–606.
[30] M. Panjan, S. Šturm, P. Panjan, M. Čekada, TEM investigation of TiAlN/CrN multilayer coatings prepared by magnetron sputtering, Surf. Coat. Technol. 202 (2007) 815–819.
[31] X. Chu, S.A. Barnett, A model of superlattice yield stress and hardness enhancements, J. Appl. Phys. 77 (1995) 4403.
[32] U. Helmersson, S. Todorova, S.A. Barnett, J.E. Sundgren, L. Markert, J.E. Greene, Growth of single-crystal TiN/VN strained-layer superlattice with extremely high mechanical hardness, J. Appl. Phys. 62 (1987) 481–484.
[33] J. Musil, Hard and superhard nanocomposite coatings, Surf. Coat. Technol. 125 (2000) 322–330.
[34] R. Hahn, M. Bartosik, R. Soler, C. Kirchlechner, G. Dehm, P.H. Mayrhofer, Superlattice effect for enhanced fracture toughness of hard coatings, Scritpa. Mater. 124 (2016) 67–70.
[35] H. Holleck, V. Schier, Multilayer PVD coatings for wear protection, Surf. Coat. Tech. 76–77 (1995) 328–336.
[36] S.J. Suresha, S. Math, V. Jayaram, S.K. Biswas, Toughening through multilayering in TiN–AlTiN films, Philos. Mag. 87 (2007) 2521–2539.
[37] B.S. Yau, J.L. Huang, H.H. Lu, P. Sajgalik, Investigation of nanocrystal-($Ti_{1-x}Al_x$)N_y/amorphous-Si_3N_4 nanolaminate films, Surf. Coat. Tech. 194 (2005) 119–127.
[38] S. Zhang, H.L. Wang, S.E. Ong, D. Sun, X.L. Bui, Hard yet tough nanocomposite coatings–present status and future trends, Plasma Process. Polym. 4 (2007) 219–228.